

Title: “Valorization of Culinary Banana Flower: Waste to Value Addition Using Green Technologies.”

Objectives:

- i) Extraction of anthocyanin from culinary banana bract and its characterization
- ii) Extraction of dietary fibre from culinary banana flower
- iii) Encapsulation of anthocyanin in dietary fibre matrix
- iv) Stability study of the encapsulated anthocyanin powder

Objective 1: Extraction of anthocyanin from culinary banana bract and its characterization

Collection and preparation of sample

Culinary banana (Musa ABB) flowers were obtained from Tezpur University Campus, Assam, India. The flower was washed with distilled water, the bract was separated from the male bud, and used for further experiments. A total of 50 g culinary banana bract was used for the experiment.

Optimization of the extraction process of anthocyanin from culinary banana bract

The bracts of culinary banana were ground using mortar and pestle with solvent: solute (5:0.5 to 15:0.5) and ethanol concentration (40–60 ml/100ml) with 0.15% of HCl. The ranges of variables were selected based on preliminary trials and the literature [1]. The ground materials were placed in an ultrasonic bath (Bandelin sonorex, Germany) with a frequency of 20 kHz and a temperature range of 40–60°C for 20 min. The extracted samples were cooled and filtered through Whatman No. 1 filter paper and kept at 4°C in the dark until further analysis.

Experimental design

Mathematical design using response surface methodology based on the parameters solvent: solute, solvent concentration, and sonication temperature was carried out. A central composite design (CCD) with three factors and one response was used for optimization of treatment condition. The best combination of solvent to solute ratio, solvent concentration, and sonication temperature was chosen.

The response (Y) was partitioned into linear, quadratic, and interactive components and the experimental data were fitted to the second-order regression equation as follows:

$$Y = b_0 + b_1X_1 + b_2X_2 + b_3X_3 + b_{11}X_1^2 + b_{22}X_2^2 + b_{33}X_3^2 + b_{12}X_1X_2 + b_{23}X_2X_3 + b_{13}X_1X_3$$

where, b_0 is the intercept; b_1 , b_2 , and b_3 are linear coefficients; b_{11} , b_{22} , and b_{33} are squared coefficients; and b_{12} , b_{23} , and b_{13} are interaction coefficients. The experimental design and statistical analysis were conducted using Design-Expert Software (Version 9, Stat-Ease, Inc. Minneapolis, MN USA). The model adequacies were checked in terms of the values of R^2 and adjusted R^2 . Analysis of variance (ANOVA) was used to determine the significance of the models. Verification of the optimized and predicted values was performed in triplicate to confirm the validity of the model.

Anthocyanin content

The total anthocyanin (TA) content was determined according to the spectrophotometric pH differential method [2]. Samples were diluted separately with 0.025 M potassium chloride buffer (pH 1) and 0.4M sodium acetate buffer (pH 4.5). Absorbance of the mixture was measured at 520 nm and 700 nm using a UV-Vis spectrophotometer. Absorbance was calculated as given in the following equation:

$$A = [(A_{520} - A_{700})_{pH1.0} - (A_{520} - A_{700})_{pH4.5}]$$

Table 1: Independent variables and their levels employed in a central composite design for the optimization of culinary banana bract extract for anthocyanin content

Variables	Low	Centre	High
Solvent: solute ratio	5	10	15
Ethanol concentration (ml/100ml)	40	50	60
Sonication temperature (°C)	40	50	60

The TA content was calculated as cyanidin-3-glucoside equivalents as shown in the following equation:

$$\text{Anthocyanin content} \left(\frac{\text{mg}}{100\text{g}} \right) = \frac{A \times MW \times DF \times V \times 100}{\epsilon \times l \times m_{\text{sample}}}$$

where, A is the absorbance, MW is the molecular weight (MW=449.2 g mol^{-1}), DF is the dilution factor, ϵ is the molar absorptivity ($\epsilon = 26900 \text{ L cm}^{-1} \text{ mol}^{-1}$), V is the volume of solvent in ml, and l is the path length.

Purification of anthocyanin

Column chromatography was used for further purification of anthocyanin. The concentrated anthocyanin extracts were diluted with distilled water and loaded onto Amberlite XAD 7N

macro pore absorptive resins. The Amberlite XAD 7N resins were washed with distilled water and the absorbed anthocyanin was recovered with 80% ethanol. To remove the ethanol and part of the water, the ethanol eluate was concentrated using a rotary vacuum evaporator and the anthocyanin extract was stored at 4°C until use.

Identification of anthocyanins by HPLC

Identification of anthocyanin by HPLC was performed following the method given by Gracia-Tejeda et al. [3] The purified anthocyanin of banana bract was identified by HPLC (Waters Corporation, USA, UV/Visible Detector-2489). The solvent system used was water, methanol, formic acid (14:5:1), and the flow rate was 1.5 ml/min. The elutes were monitored by visible spectrometry at maximum wavelength 530 nm.

Properties of purified anthocyanin extract

Hygroscopicity

The hygroscopicity of purified anthocyanin extract was determined according to Cai and Corke [4] and Tonon et al. [5] with modifications. Samples from each powder were stored at room temperature in a desiccator containing saturated sodium chloride (NaCl) solutions (75% RH; Aw = 0.75). The samples were weighed after one week, and the hygroscopicity was expressed in grams of absorbed moisture per 100 g of dry solids.

Solubility

Solubility of purified anthocyanin extract was determined according to the method of Singh and Singh [6]. Powder suspension of 1 g/100 ml was agitated for 30 min in a shaker and then it was centrifuged at 3000 rpm for 10 min. The supernatant obtained was deposited in petriplate and subjected to a temperature of 110°C for 4 h in a drying oven. The solubility was calculated according to the following equation:

$$\text{Solubility}(S) = \{(\text{Grams of supernatant solids} \times 4) \times 100\} \div (\text{Grams of sample})$$

Results and discussion

Optimization of the UAE process

A CCD was developed for extraction of TA from the bract of culinary banana using sonication. Multiple regression analysis was performed based on the experimental values, and second-order polynomial model represents the recoveries of anthocyanin. A final predictive equation was developed after neglecting the non-significant terms ($p > 0.05$). The quality of the fit of the model was expressed by the R^2 correlation coefficient (0.934), and its statistical significance was

confirmed with an F-test. Results were found significant ($p < 0.001$), attesting to the goodness of fit of the models and lack of fit was insignificant ($p > 0.05$) and it further confirmed model validity. Regression coefficients of the models for anthocyanin obtained by the multiple linear regressions are presented. Three-dimensional response surface plots were constructed to predict the effects of the independent variables and their mutual interaction on the response variables. The values of the coefficients for anthocyanin were used for a final predictive equation as follows:

$$Y = 55.19 + 3.95X_1 + 2.61X_2 + 0.12X_3 - 0.16X_1X_2 - 0.72X_1X_3 + 1.13X_2X_3 - 2.27X_1^2 - 2.43X_2^2 - 1.28X_3^2$$

Based on the above equation, three-dimensional plots represented the effects of extraction process variables on the anthocyanin from culinary banana bract. As shown by Dranca et al., [7] ultrasound assistance improved anthocyanin extraction, which is attributed to its cavitation phenomena and maximum extraction efficiency at ultrasonic frequency 37.5 kHz. Ultrasonics has a linear positive effect on the extraction of polyphenols and anthocyanins from *A. melanocarpa* by-products [8]. However, a known deleterious effect on the active constituents of medicinal plants through the formation of free radicals and consequently undesirable changes in the drug molecules were found at ultrasound energy (> 20 kHz) [9]. In the present study, the sonication frequency was kept constant at 20 kHz and the effect of other parameters on anthocyanin yield at this ultrasonic frequency was observed. Solvent concentration and solvent solute ratio had a stronger effect in the extraction of anthocyanin. There was a linear increase in the TA content with increase in solvent solute ratio at constant ethanol concentration. A larger solvent volume can dissolve the constituents more effectively and thus result in improvement of the extraction yield [10]. A similar effect of ethanol concentration on anthocyanin was observed. The combination of temperature with ultrasonic frequency plays an important role in determining the anthocyanin yield. Increase in sonication temperature at constant solvent solute concentration resulted in an increase in the anthocyanin content up to a certain limit of the tested range. However, further increase of extraction temperature resulted in a decrease of the TA content. There was a linear increase in TA with the increase of sonication temperature at a fixed extraction concentration up to a certain limited range, while a rise in ethanol concentration at a fixed extraction temperature also led to a marked increase in TA. Similar linear and quadratic

effects of extraction variables in UAE of anthocyanin from mulberry were also observed by Zou et al. [1].

Optimum extraction conditions

Based on our findings, the predicted UAE conditions were 15:0.5 solvent to solute ratio, 53.97 ml/100ml ethanol concentration, and 49.39°C temperature for the TA (57.29 mg/100g). The R^2 value of the model was 0.934, R^2 -adjusted value was 0.876, F value was 15.91, and the p-value was < 0.0001 , which represent that the model had adequately represented the actual relationship among the parameters chosen. Under the above-mentioned conditions, the experimental TA content (56.98 mg/100g) agreed well with the predicted value.

Identification of anthocyanins by HPLC

Anthocyanins pigments extracted from culinary banana bract were separated and identified by HPLC. The results revealed the detected types of anthocyanin pigments from culinary banana bract viz., cyanidin-3-O-glucoside (peak 2) and peonidin-3-O-glucoside (peak 5) and represented 4.86% and 7.17% of the total area, respectively. However, the intense peak 4 may be ascribed to cyanidin-3-rutinoside based on the literature [11].

Hygroscopicity

The hygroscopicity of the encapsulated pigment powder was found to $28.89 \pm 0.09\%$. Similar results were also observed in spray-dried blackberry juice using maltodextrin 20DE with inlet temperatures of 160°C and 180°C and ranged from 28.73% to 29.51% [12], whereas slight variation was observed in barberry anthocyanins with maltodextrin as the wall material [13]. The hygroscopicity values inversely increased with moisture content such that a lower powder moisture content indicated higher hygroscopicity [14].

Solubility

The solubility of the encapsulated powder was found to be $84.10 \pm 0.20\%$. Maltodextrin of different dextrose equivalent (DE) is commonly used because of its higher water solubility and it contains more hydrophilic group because of the lower molecular weight [15]. Solubility of the encapsulated anthocyanin with maltodextrin (10 DE) varied (82.79–87.42%) with inlet air temperature from 140°C to 180°C and the highest powder solubility (87.42%) and dispersibility (86.45%) were observed at 180°C inlet air temperature, which are in line with the present study [16].

Objective 2: Extraction of dietary fibre from culinary banana flower

Extraction of dietary fibre from dried culinary banana bract

The dried culinary banana bract (CBB) was deoiled using n-hexane. The CBB was mixed with n-hexane (1:4, w/v) and stirred at 150 rpm for 15 min. Then, it was centrifuged at 4000 rpm for 20 min. The residue was dried at 50°C to obtain deoiled culinary banana bract (CBB).

DF extraction using alkaline extraction method was done according to the method described by Ma and Mu [17] with slight modification. To extract DF using alkaline extraction method, deoiled CBB was suspended in 0.5M NaOH solution (1:25, solute/solvent) and stirred at an agitation speed of 500 rpm using laboratory stirrer (RQT-127D, Remi, Maharashtra, India) for 30 min at 50°C. Then the mixture was neutralized using 0.5M HCl. The mixture was dried for 12 hrs at 40°C to obtain DF using alkaline extraction method (alkaline extracted DF, AEDF).

To extract DF using combined alkaline and ultrasound-assisted extraction method, firstly, deoiled CBB was suspended in 0.5M NaOH solution (1:25, solute/solvent) and stirred at an agitation speed of 500 rpm using laboratory stirrer (RQT-127D, Remi, Maharashtra, India) for 30 min at 50°C. Further it was sonicated at 20 kHz for time 20 min at temperature 80°C using at 50 % amplitude using probe type ultrasonicator (Q700-220 DSGitalSonicator, Qsonica LLC, USA). Then the mixture was neutralized using 0.5M HCl. The extracted DF under optimum extraction condition was then dried at 40°C overnight to obtain combined ultrasound-assisted and alkaline extracted DF (ultrasound-assisted extracted DF, UEDF).

Analysis of chemical composition

Moisture, protein, ash and crude fat content of deoiled CBB and extracted DF were determined following AOAC [18]. Enzymatic-gravimetric method was used to estimate insoluble, soluble and total DF [19]. The mineral contents of deoiled CBB and extracted DF were quantified using Atomic absorption spectrophotometer (Thermo Scientific, ICE 3000 Series, Newington, USA)

Phenolic analysis of extracted DF by GC-MS

The extraction phenolics of deoiled CBB, AEDF and UEDF were described. The extracts was derivatized by treating BSTFA (with 1% TMCS) and anhydrous pyridine (1.5 mL, 1:1). The mixture was heated for 1 h at 90°C and the trimethylsilylated derivatives were analyzed in GC-MS (Agilent 240 Ion Trap GC/MS, USA) using capillary column (HP-5). Initially, column temperature was held at 80°C for 1 min, then programmed to 220°C at a rate of 10°C /min, and

then 220 to 310°C at a rate of 20°C/min with a final hold time of 6 min. Injector temperature was maintained at 280 °C. Mass spectra were scanned from m/z 50 to 650 at a rate of 1.5 scans/s.

FT-IR analysis of extracted DF

The functional groups present in deoiled CBB and extracted DF (UEDF and AEDF) were determined using spectrometer (Nicolet Instruments 410 FTIR, Thermo Scientific, USA). Spectra were attained over the range of 400-4000 cm⁻¹ with 4 cm⁻¹ resolution and 16 scans were collected.

XRD analysis of extracted DF

The crystallinity of the deoiled CBB, UEDF and AEDF were determined using X-ray Diffractometer (Bruker AXS, Bruker D8 FOCUS, Germany) operated at 60 kV. The analysis was performed at 2θ range of 5-80° and a scan rate of 2.0°/min. The degree of crystallinity [20] was calculated as below:

$$D_c(\%) = \frac{A_c \times 100}{A_c + A_a}$$

Where, D_c is the degree of crystallinity; A_c is crystallized area and A_a is amorphous area on X-ray diffractogram

SEM analysis of extracted DF

The microstructure and surface morphology of deoiled CBB, UEDF and AEDF were examined by SEM (JSM-6390LV, JEOL, Japan), operated at 20kV and 1500X magnification.

TGA analysis of extracted DF

The thermal analysis of deoiled CBB, UEDF and AEDF was conducted using thermogravimetric analysis (NETZCH TG 209F1 Libra, Germany) according to the method described in Zhang et al. [21] with slight modifications. The TGA was performed under nitrogen atmosphere and temperature ranged from 25° C to 400°C at a rate of 10°C/min.

Particle size distribution of extracted DF

The particle size distribution of UEDF and AEDF along with deoiled CBB was done using particle size distribution analyzer equipped with dynamic light scattering (DLS) system (Microtrac Nanotrac Wave, MN401, USA). Deionized water was used for dispersion of the samples.

GC-MS analysis of UEDF for monosaccharide composition

UEDF was dissolved in 2M trifluoroacetic acid (TFA) (30 mL) and hydrolyzed for 3h at 120°C. The content was centrifuged at 4000 rpm for 15 min and the TFA in the supernatant was evaporated off. The released monosaccharide was derivatized according to the method described by Guentas et al. [22]. The hydrolysate (200 µg) was dissolved in 200 µL pyridine and derivatized using trimethylsilylated reagent (200 µL BSTFA with 1% TMCS). The trimethylsilylated derivatives were analyzed in GC-MS (Agilent 240 Ion Trap GC/MS, USA) using capillary column (HP-5). The programme used for analysis was as mentioned in the method by Ly et al. [23].

The program used for analysis was: injection temperature and detector temperature were both set at 230°C; column temperature was programmed from 130 to 180°C at 2°C /min, holding at 180°C for 3 min, then increased to 220°C at 10°C /min. Final holding temperature was at 220°C for 3 min. Carrier gas was helium. The split ratio was set to 10:1. Injection volume of sample was 10 µL.

Functional properties of extracted DF

To determine the water holding capacity (WHC) and oil holding capacity (OHC), method followed was according to Rodríguez et al. [24]. Water swelling capacity (WSC) was calculated as stated by Robertson et al. [25].

Glucose absorption capacity (GAC) was determined following the method of Peerajit et al. [26]. GAC was calculated using following equation

$$GAC \left(\frac{mmol}{g} \right) = (C_i - C_s) \times \frac{V_i}{W_s}$$

Where, C_i is initial glucose concentration in mmol/L; C_s is glucose concentration of supernatant when absorption of glucose reached maximum in mmol/L; V_i is the volume of supernatant in mL; W_s is weight of DF in g.

α -amylase inhibition ratio (α -AAIR) was determined following the method described by Ahmad et al. [27] and calculated using following equation

$$\alpha - AAIR (\%) = \frac{(A_c - A_s) \times 100}{A_c}$$

Where, A_c is absorbance of control; A_s is absorbance of DF

Statistical analysis

The data were statistically analyzed using SPSS 16. Means of data obtained were evaluated by analysis of variance (ANOVA) with Duncan's multiple range tests to identify significant differences ($p < 0.05$).

Results and discussion

Changes in chemical composition of extracted DF

The chemical composition and mineral content of deoiled CBB, UEDF and AEDF were determined. TDF content of UEDF (83.38g/100g) was significantly higher compared to deoiled CBB and AEDF. Moreover it is higher than that of mango (74g/100g), lemon (70.76 g/100g) and yellow passion fruit (71.79g/100g) [28]. Deoiled culinary banana bract (CBB) contains slightly higher fat value than other treatment. For AEDF and UEDF, the deoiled CBB was further processed using alkaline and ultrasound treatment which results in the reduction of fat value. However, the high intensity ultrasound in UEDF results in protein denaturation [29]. Protein and starch content of UEDF is lesser when compared to deoiled CBB and AEDF. The ash content of AEDF and UEDF decreased from the deoiled CBB which could be evident from the decrease in mineral contents.

Table 2: Chemical composition of deoiled CBB, UEDF and AEDF

Composition	Deoiled CBB	UEDF	AEDF
Moisture (g/100g)	10.36±0.04 ^c	9.82±0.28 ^a	10.21±0.06 ^b
Fat (g/100g)	1.32±0.08 ^c	0.98±0.01 ^a	1.08±0.14 ^b
Protein (g/100g)	1.85±0.05 ^c	1.06±0.06 ^a	1.55±0.10 ^b
Ash (g/100g)	11.36±0.03 ^c	6.23±0.06 ^a	7.16±0.06 ^b
Starch (mg/100g)	9.06±0.12 ^c	4.32±0.11 ^a	5.68±0.19 ^b
IDF (g/100g)	69.35±0.69 ^a	78.73±0.14 ^c	75.43±0.46 ^b
SDF (g/100g)	4.51±0.04 ^a	4.65±0.02 ^b	4.68±0.28 ^c
TDF (g/100g)	73.86±0.70 ^a	83.38±0.20 ^c	80.11±0.70 ^b
K (mg/100g)	1882.60±0.06 ^c	724.11±0.02 ^a	1020.62±0.24 ^b
Ca (mg/100g)	763.33±0.20 ^c	630.74±0.35 ^a	658.06±0.05 ^b
Mg (mg/100g)	300.07±0.06 ^c	182.62±0.04 ^a	243.01±0.11 ^b
Fe (mg/100g)	25.11±0.11 ^c	15.00±0.02 ^a	19.10±0.10 ^b

*(Mean with different superscript letters in the same row represent a significant difference at $p < 0.05$, values represent mean ± SD; n=3) *IDF-insoluble DF; SDF-soluble DF; TDF-total DF

Phenolics of extracted DF

Five different phenolic derivatives were identified in deoiled CBB viz., (1) Benzoic acid trimethylsilyl ester, (2) 3,4-Dimethyl benzoic acid, (3) Phenol, 2,5-bis (1,1-dimethylethyl), (4) 4-Methoxycinnamic acid, and (5) Anthraquinone. Benzoic acid is the precursor of naturally occurring phenolic acid i.e., hydroxyphenolic acid [30]. Phenolic compounds are classified as simple phenols or polyphenols based on the number of phenol units in the molecule. Phenol, 2, 5-bis (1,1-dimethylethyl) is also known as 2,5-Di-tert-butylhydroxybenzene. 4-methoxycinnamic acid is a methoxycinnamic acid having a single methoxy substituent at the 4-position on the phenyl ring. It derives from a cinnamic acid [31]. Anthraquinone is the most important quinone derivative of anthracene. Moreover, it is the parent substance of a large class of dyes and pigments. Three phenolic derivatives were identified in AEDF extract namely, (1) Benzoic acid trimethylsilyl ester, (2) Phenol, 2, 5-bis (1,1-dimethylethyl), (3) Cinnamic acid. Cinnamic acid is a precursor in the formation of other more complex phenolic compounds. Four phenolics were identified in AEDF (1) 2-Methoxy-4-vinylphenol, (2) Phenol, 2,4-di-tert butyl, (3) 2-tert-Butyl-4-methoxyphenol, and (4) Cinnamic acid. 2-Methoxy-4-vinylphenol is an aromatic substance used as a flavoring agent. It is a derivate of ferulic acid [32].

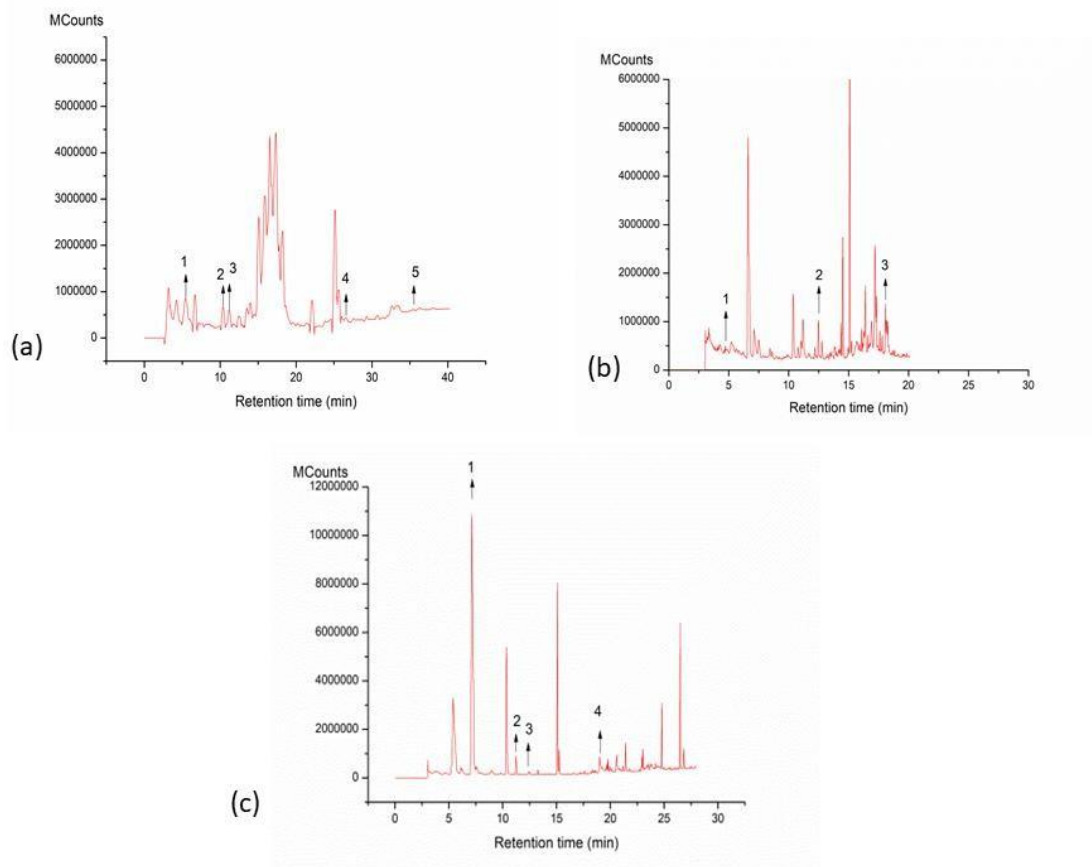


Fig. 3.1. (a) GC Chromatogram of phenolics of deoiled CBB (1)Benzoic acid trimethylsilyl ester, (2) 3,4-Dimethyl benzoic acid, (3) Phenol, 2,5-bis (1,1-dimethylethyl), (4) 4-Methoxycinnamic acid, (5) Anthraquinone; (b) UEDF (1)Benzoic acid trimethylsilyl ester, (2) Phenol, 2,5-bis (1,1-dimethylethyl), (3) Cinnamic acid and (c) AEDF (1) 2-Methoxy-4-vinylphenol,(2)Phenol, 2,4-di-tert butyl, (3)2-tert-Butyl-methoxyphenol, and (4) Cinnamic acid

FT-IR analysis of extracted DF

The FT-IR spectra of deoiled CBB, UEDF and AEDF shows a broad peak at 3410 and a minor peak at 2925 cm^{-1} resembled to O-H stretching of hydrogen attached to hydroxyl group and C-H stretching of methylene group in polysaccharide, respectively [33]. Thus, these peaks indicate structure of cellulose and hemicelluloses. Peaks at 1639 and 1434 cm^{-1} are responsible for aromatic hydrocarbons of lignin and CH_2 stretching of cellulose, respectively. Moreover, the peak at 1049 cm^{-1} corresponded to C-O stretch bond and it indicated breakdown of

oligosaccharides from insoluble DF (IDF) [33]. Presence of all these groups confirmed the typical polysaccharide structure of UEDF and AEDF along with the deoiled CBB.

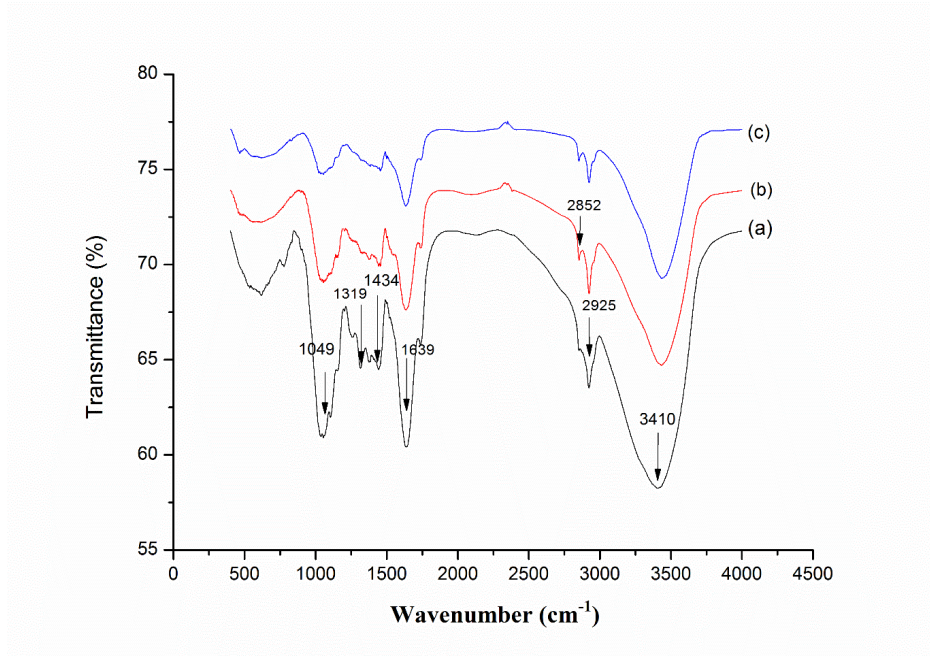


Fig.3.2. FT-IR spectrum of (a) Deoiled CBB, (b) UEDF and (c) AEDF

Microstructure changes in extracted DF

Surface morphology of deoiled CBB, UEDF and AEDF were observed. For deoiled CBB, the network structure was started to form whereas a well separated fibrous network can be seen in case of AEDF. A typical honeycomb structure can be seen for UEDF and it was attributed to ultrasound treatment which make large pore in the cell wall and loosening of the bond between fibrils. Shear emulsifying treatment in combination with enzymatic hydrolysis also results in more regular honeycomb pore for DF extracted from deoiled cumin [17].

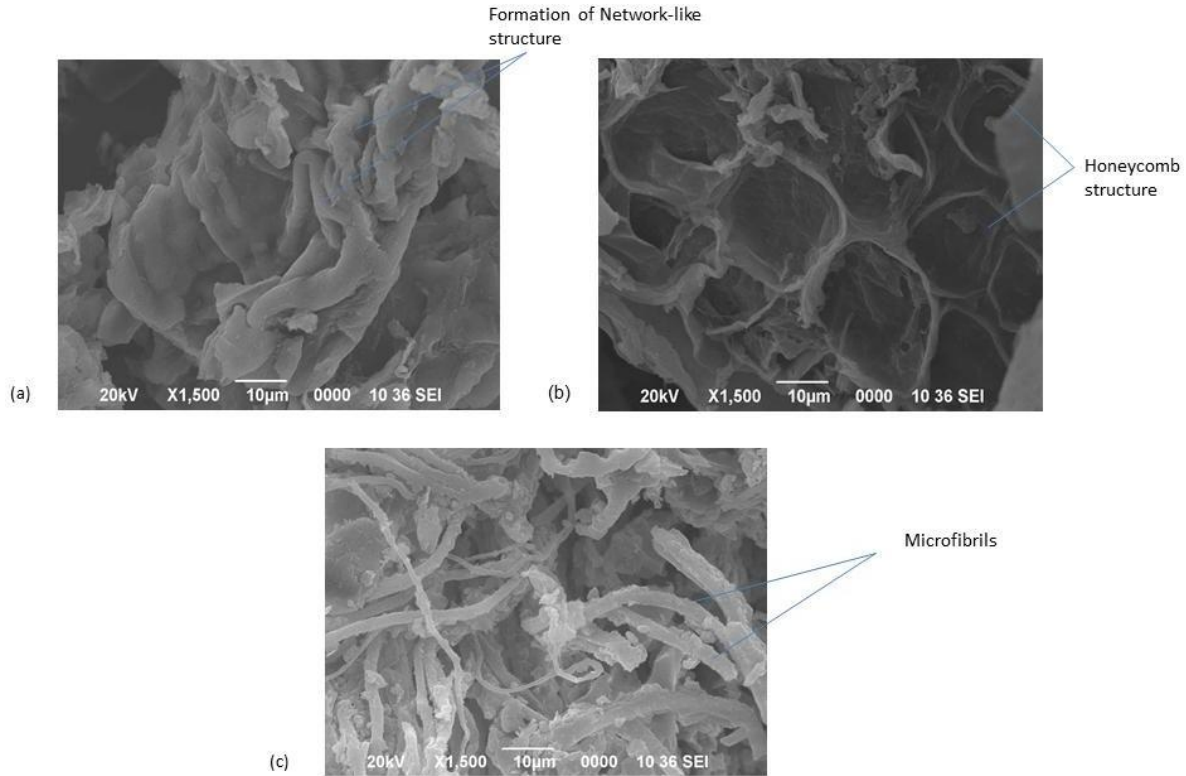


Fig.3.3. SEM micrograph of (a) Deoiled CBB, (b) UEDF and (c) AEDF

XRD analysis of extracted DF

The crystallinity of deoiled CBB, UEDF, and AEDF was determined from X-ray diffraction chromatogram. The prominent peak detected at 2θ (22°) and minor peaks at 2θ (15° and 33°), confirmed the presence of crystalline region. The crystallinity of UEDF (25.86%) was significantly higher compared to deoiled CBB (13.97%) and AEDF (25.02%). High intensity ultrasound treatment led to hydrolysis of hemicelluloses and removal of amorphous portion of cellulose which resulted in increased crystallinity.

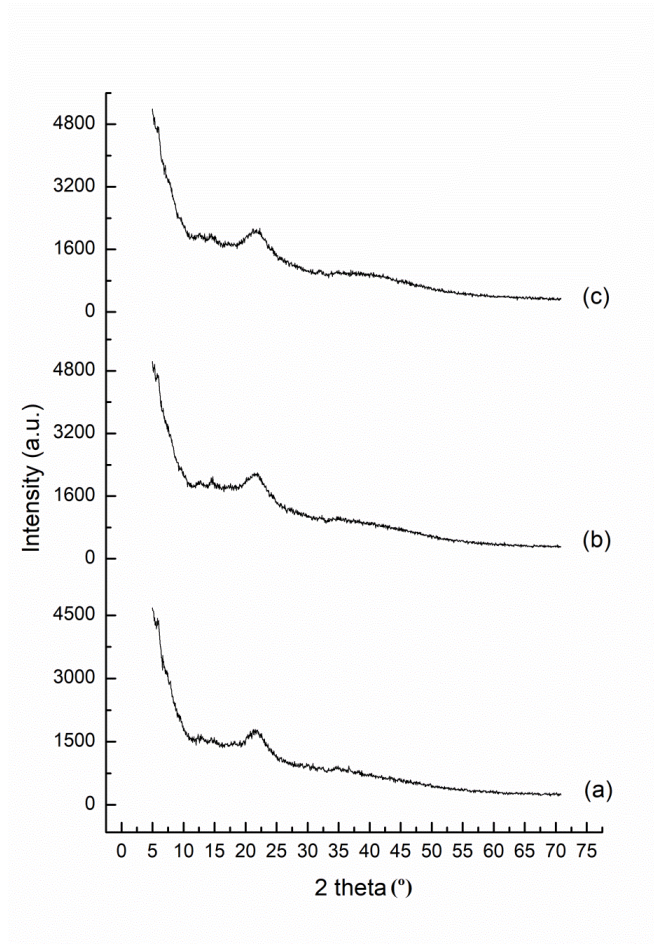


Fig.3.4. XRD analysis of (a) Deoiled CBB, (b) UEDF and (c) AEDF

TGA analysis of extracted DF

Thermal stability of a polymer is an important property when the polymer is thermally processed or used for baking. The TGA graphs for deoiled CBB, UEDF and AEDF depicts that weight loss occurred in three different temperature ranges (25-190°C, 190-310°C, and 310-400°C). Devolatilization occurred at around 120°C which was due to evaporation of absorbed water [17]. The second and third temperature ranges indicated depolymerization of hemicelluloses and cellulose degradation [34]. The weight loss (%) of UEDF was least (56.08%) and hence it was more thermally stable compared to deoiled CBB and AEDF. Ultrasonicated lignin and cellulose also showed higher thermal stability than sample without ultrasonic treatment [35].

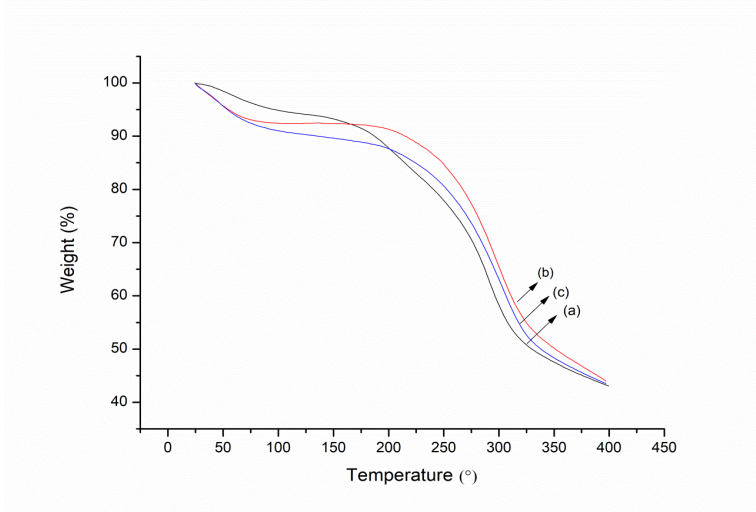


Fig. 3.5. TGA analysis of (a) Deoiled CBB, (b) UEDF and (c) AEDF

Particle size distribution of extracted DF

The particle size distribution of deoiled CBB, UEDF and AEDF based on dynamic light scattering (DLS) illustrated that the mean particle size of deoiled CBB was less than $1\mu\text{m}$ and AEDF was approximately $0.5\mu\text{m}$. More uniform and lesser particle size distribution with mean particle size less than $0.5\mu\text{m}$ compared to the deoiled CBB and AEDF. The high intensity ultrasound treatment disintegrates fibres into thinner, shorter and uniform size particles [34]. Thus, the surface area increased as it depends on the size of particles. The increased surface area is responsible for improving functional properties [36].

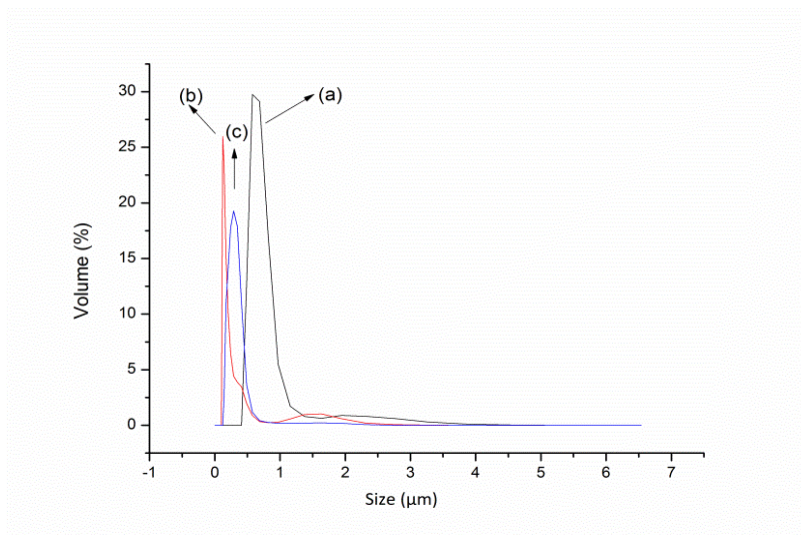


Fig. 3.6. Particle size distribution of (a) Deoiled CBB, (b) UEDF and (c) AEDF

Monosaccharide composition of UEDF

The monosaccharides were identified by comparison of mass spectrum data for the compounds (NIST, version 2.0). The MS analysis of ion showed similar mass spectrum for compound 1 (5-hydroxymethylfurfural) which was formed by dehydration of 6-carbon sugar (hexoses) [37]. Hydroxymethylfurfural (HMF) is formed mainly by the dehydration of monosaccharides which required the loss of three water molecules. Antal et al. [38] reported the decomposition of fructose in water at high temperatures with the formation of possible side products and HMF. Fructose forms equilibrium mixtures of difructose and dianhydrides, and thus resulted in formation of HMF. However, β -D-glucopyranose was identified as compound 2.

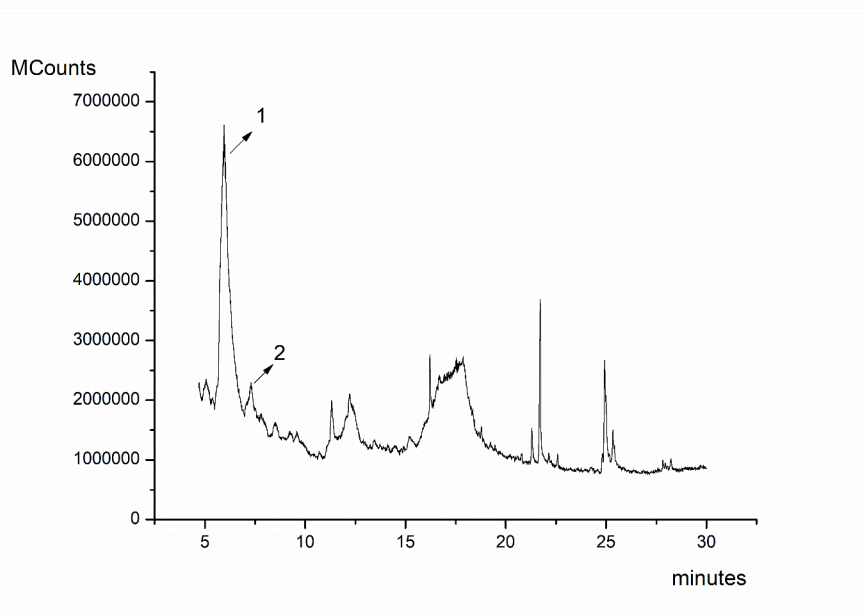


Fig.3.7(a). Chromatogram of monosaccharide composition of UEDF (1) 5-Hydroxymethylfurfural; (2) β -D-Glucopyranose

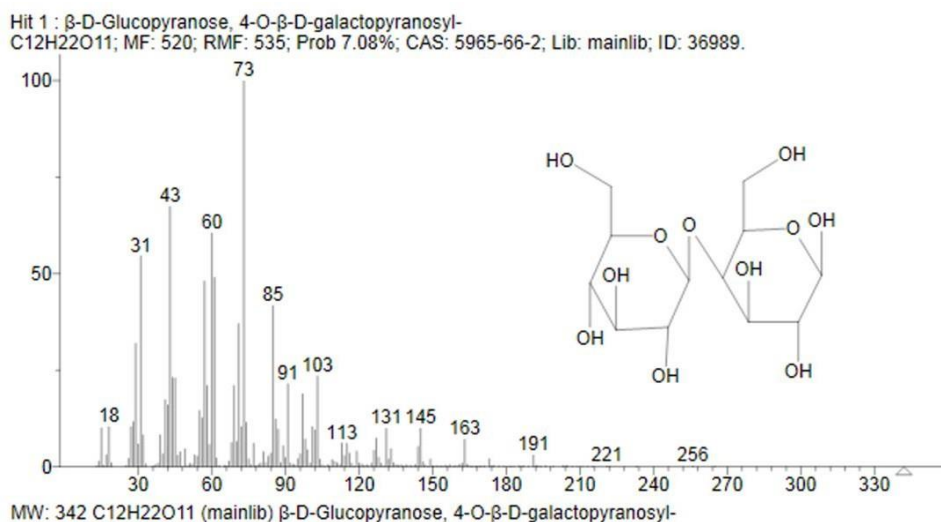
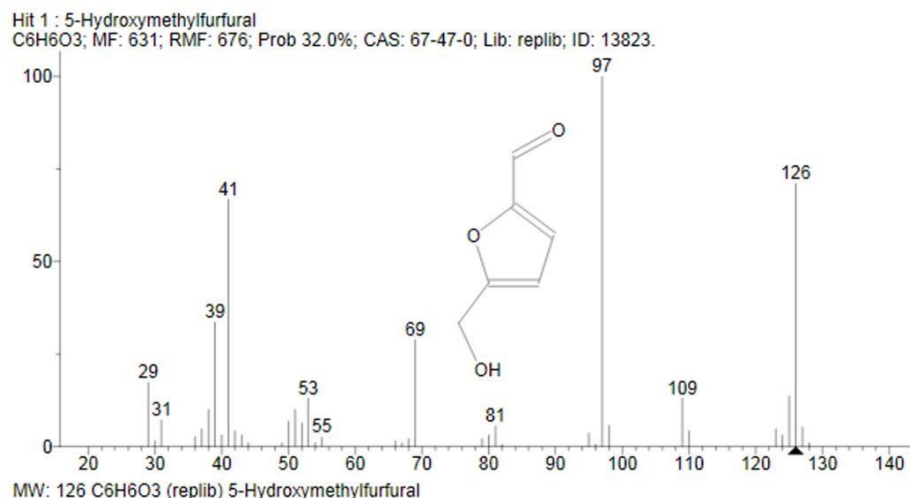


Fig. 3.7 (b). MS spectra of compound 1 (5-Hydroxymethylfurfural) and compound 2 (β-D-Glucopyranose)

Functional properties of extracted DF

The WHC, OHC and WSC of UEDF were 12.73g water/g sample, 7.83g oil/g sample, and 15.84 mL/g, respectively. It was significantly higher when compared to deoiled CBB and AEDF. The WHC was higher than that of citrus fruits (1.65g/g), apple (1.87g/g), mango peel (11.40g/g) and coconut kernels (10.71g/g) [39]. The increase in WHC depends on decrease in particle size, porosity, surface and microstructure [40]. The OHC was also found higher than that of citrus fruits, grapes and apple DF. The WSC of UEDF was higher as compared to peas (5.76 mL/g), edible seaweed (5.7-10.5mL/g) [41]. Interaction of DF with water occurs via two mechanisms

i.e., (i) holding of water in capillary structure due to surface tension strength, (ii) holding of water through hydrogen bond and dipole form. The higher WSC was attributed to particle size distribution, surface characteristics, chemical composition (TDF and SDF content) [42]. The high intensity ultrasound treatment resulted in reduction of particle size and increased surface area. Moreover, it also resulted in formation of network structure of DF and exposed the free polar groups which in turn contributed to high WSC.

The α -AAIR was increased significantly for UEDF (31.20 %) and higher than DF extracted from cumin (13.64-21.84%). The increase in α -AAIR was due to reduction in particle size and increase in crystalline structure of cellulose. Hence, α -amylase was absorbed by DF and starch molecules get entrapped in the fibrous network. Thus, the contact between α -amylase and starch got inhibited and decreased the amount of glucose in serum. For GAC, no significant changes was observed at glucose concentration 50 mmol/L among deoiled CBB, UEDF, and AEDF. However, the glucose concentration at 200 mmol/L, the GAC of UEDF was found to be 16.33 mmol/g. The GAC of UEDF was significantly higher as compared to deoiled CBB and AEDF. The GAC of DF extracted from cumin was 2.02-60.86 mmol/g [17]. Higher GAC was attributed to smaller particle size and physical structure of fibre where glucose molecule get entrapped and thereby reducing its release [26].

Table 3: Functional properties of deoiled CBB, UEDF and AEDF

Functional properties	Deoiled CBB	UEDF	AEDF
WHC (g water/g dry sample)	9.79±0.19 ^a	12.73±0.13 ^c	10.67±0.12 ^b
OHC (g oil/g dry sample)	6.94±0.05 ^a	7.83±0.28 ^b	6.96±0.05 ^a
WSC (mL/g)	10.23±0.28 ^a	15.84±0.46 ^c	14.81±0.31 ^b
α AAIR (%)	18.32±0.14 ^a	31.20±0.26 ^c	23.14±0.34 ^b

Objective 3: Encapsulation of anthocyanin in dietary fibre matrix

Preparation of DF-anthocyanin formulation

Purified anthocyanin extract was mixed with DF with different ratio (2:1 to 4:1) and were homogenised. The TSS of the mixture was adjusted to 20° Brix. The preparation was then freeze dried (Lyolab_3S, Lyophilization System India Pvt Ltd Hyderabad, India). The anthocyanin-fibre preparation with different anthocyanin and DF as matrix ratio were named as DF-A2 (2:1), DF-A3 (3:1) and DF-A4 (4:1). A control without anthocyanin was prepared and named as DF-C. Cellulose was used as a replacement for DF and was coded as CEL-A.

Physicochemical analysis

Moisture content of DF-anthocyanin formulation was determined according to the method described in AOAC [43].

The total anthocyanin (TA) content of formulation was determined according to the spectrophotometric pH differential method [2]. The TA content was calculated as cyanidin-3-glucoside equivalents. Absorbance was calculated as given in the following equation

$$A = [(A_{520} - A_{700})_{\text{pH 1.0}} - (A_{520} - A_{700})_{\text{pH 4.5}}]$$

The total anthocyanin content was calculated as cyanidin-3-glucoside equivalents as shown in the following equation

$$\text{Anthocyanin content } \left(\frac{\text{mg}}{100\text{g}} \right) = \frac{A \times MW \times DF \times V \times 100}{\epsilon \times l \times m_{\text{sample}}}$$

where, A is the absorbance; MW is the molecular weight (MW=449.2 gmol⁻¹); DF is the dilution factor; ϵ is the molar absorptivity ($\epsilon = 26900 \text{ Lcm}^{-1}\text{mol}^{-1}$); V=volume of solvent in ml; l is the path length.

DPPH free radical scavenging activity of formulation was determined following the method of Brand-Williams et al. [44]

The hygroscopicity of the formulation were determined according to Cai and Corke [4] and Tonon et al. [5].

Color characteristics of DF-anthocyanin formulation

L*, a*, and b* colour values of the formulated powder were measured using a Hunter Color Measurement Spectrophotometer (UltraScan VIS, Hunter Lab) after equipment standardization. Chroma (C*) and hue angle (H°) was determined using the following equations:

$$C^* = \sqrt{a^{*2} + b^{*2}}$$
$$H^{\circ} = \tan^{-1} \frac{b^*}{a^*}$$

FT-IR analysis of extracted DF-anthocyanin formulation

The characterization and functional groups of DF-anthocyanin formulation were determined using spectrometer (Nicolet Instruments 410 FTIR, Thermo Scientific, USA). Spectra were attained over the range of 400-4000 cm⁻¹ with 4 cm⁻¹ resolution and 16 scans were collected.

XRD analysis of extracted DF-anthocyanin formulation

The crystallinity of DF-anthocyanin formulation were determined using X-ray Diffractometer (Bruker AXS, Bruker D8 FOCUS, Germany) operated at 60 kV. The analysis was performed at 2θ range of 5-80° and a scan rate of 2.0°/min. The degree of crystallinity [20] was calculated as below:

$$D_c(\%) = \frac{A_c \times 100}{A_c + A_a}$$

Where, D_c is the degree of crystallinity; A_c is crystallized area and A_a is amorphous area on X-ray diffractogram

SEM analysis of DF-anthocyanin formulation

The structural and morphological features of DF-anthocyanin formulations were analysed by JSM-6390LV (JEOL, Japan) scanning electron microscope. SEM was operated with 20kV at magnification of 750X and 3000X.

Analysis of fluorescence property of DF-anthocyanin formulation

The samples were prepared by dissolving in Milli-Q water (2×10⁻⁵ mol dm⁻³) at pH 5.5. The pH is chosen according to the procedure of Drabent et al. [45]. The fluorescence emission spectra were recorded (25.0±0.2°C) using a fluorescence spectrophotometer (Perkin Elmer, LS 55, Singapore). The excitation wavelength used was 220 and 270 nm.

Storage study

The formulated powder was stored under accelerated storage condition at 35°C and 75% RH. Samples were analysed at every 7-day interval for anthocyanin content. The reaction rate constant (k) and half-lives ($t_{1/2}$) were calculated for all three reaction kinetic model using the following equations

Zero-order reaction kinetic model

$$C_t = C_0 - kt$$

$$t_{\frac{1}{2}} = \frac{C_0}{2k}$$

First-order reaction kinetic model

$$C_t = C_0 \exp(-kt)$$

$$t_{\frac{1}{2}} = \frac{\log 2}{k}$$

Second-order reaction kinetic model

$$\frac{1}{C_t} - \frac{1}{C_0} = kt$$

$$t_{\frac{1}{2}} = \frac{1}{k} \times \frac{1}{C_0}$$

C_0 is the initial anthocyanin content, C_t is the anthocyanin content at reaction time t and k is the reaction rate

$t_{1/2}$ is the time when the anthocyanin content was reduced by 50 % with respect to zero time [46]. Three reaction kinetic models were applied to data and based on the best fits (higher R^2), the kinetic model was selected for the storage study.

Statistical analysis

Experiments were carried out in triplicate. Means of data obtained were evaluated using Duncan's multiple range test to identify significant differences at the 0.05 probability ($p < 0.05$) using the SPSS 16.

Results and discussion

Anthocyanin content of DF-anthocyanin formulations increased significantly with the increase of pigment-matrix ratio and it was highest in DF-A3. The anthocyanin content decreased in DF-A4 due to inadequate amount matrix as compared to the pigment [14]. The total anthocyanin content in CEL-A was lesser relative to DF-anthocyanin formulation. The antioxidant content was found to be highest in DF-A3 which was related to high anthocyanin content. For CEL-A, the

antioxidant content was 0.36 $\mu\text{mol TE/g}$ fresh mass which was lesser relative to other DF-anthocyanin formulations. Hygroscopicity did not follow any special trend and varied from 7.01-12.11 %. Hygroscopicity was significantly higher in CEL-A compared to the DF-anthocyanin formulations.

Table 4: Physicochemical properties of DF-anthocyanin formulation

	DF-C	DF-A2	DF-A3	DF-A4	CEL-A
Moisture content (g/100g)	8.57 \pm 0.05 ^a	8.9 \pm 0.61 ^b	9.21 \pm 0.12 ^c	9.56 \pm 0.30 ^d	10.4 \pm 0.23 ^e
Total anthocyanin (mg/100g)	3.39 \pm 0.23 ^a	15.24 \pm 0.25 ^b	41.64 \pm 0.13 ^e	28.41 \pm 0.08 ^d	18.38 \pm 0.15 ^c
DPPH ($\mu\text{mol TE/g}$ fresh mass)	0.07 \pm 0.08 ^a	0.57 \pm 0.02 ^c	1.33 \pm 0.15 ^e	1.11 \pm 0.07 ^d	0.36 \pm 0.02 ^b
Hygroscopicity (%)	7.78 \pm 0.12 ^b	7.01 \pm .22 ^a	8.71 \pm 0.16 ^c	9.29 \pm 0.15 ^d	12.11 \pm 0.8 ^e

*(Mean with different superscript letters in the same row represent a significant difference at $p < 0.05$, values represent mean \pm SD; n=3)

Color characteristics of formulated powder

The color characteristics of DF-anthocyanin formulation was shown to have L* value increased with the pigment content up to DF-A3 and then again decreased. Chroma (C*) was comparatively higher in DF-A4 among the DF-anthocyanin formulations. Chroma (C*) was found to be highest in CEL-A as the higher b* value of DF influenced the bright purple colored pigment.

Table 5: Color characteristics of DF-anthocyanin formulation

Sample code	Colour values				
	L*	a*	b*	C*	H°
DF-C	44.43±0.07 ^a	6.8±0.12 ^a	10.02±0.31 ^c	12.10 ^b	55.83 ^d
DF-A2	46.32±0.22 ^b	7.76±0.21 ^b	9.18±0.05 ^d	12.02 ^a	49.79 ^c
DF-A3	50.42±1.19 ^d	9.12±0.12 ^c	8.14±0.24 ^b	12.22 ^c	41.75 ^b
DF-A4	48.72±0.52 ^c	9.27±0.16 ^d	8.27±0.20 ^c	12.42 ^d	41.73 ^b
CEL-A	64.31±1.16 ^e	15.15±0.17 ^e	1.23±0.32 ^a	15.19 ^e	4.64 ^a

*(Mean with different superscript letters in the same column represent a significant difference at $p < 0.05$, values represent mean \pm SD; n=3)

FT-IR analysis of DF-anthocyanin formulation

The functional group of DF-anthocyanin formulation along with the anthocyanin extract were analysed by FT-IR. The absorption band at 3434, 2925, 1634, 1447 and 1049 cm^{-1} in all the formulations, confirmed the typical polysaccharide structure [47]. However peak at 1516, 1261 and 1072 cm^{-1} corresponds to vibrational stretching of aromatic rings (=C-O-C group) in flavonoids were observed in the anthocyanin extracts [48]. The individual bands were seen in all the formulations. As reported by Khor et al. [49], an unchanged structure of quercetin was observed in quercetin-fibre formulations before and after nanoformulation.

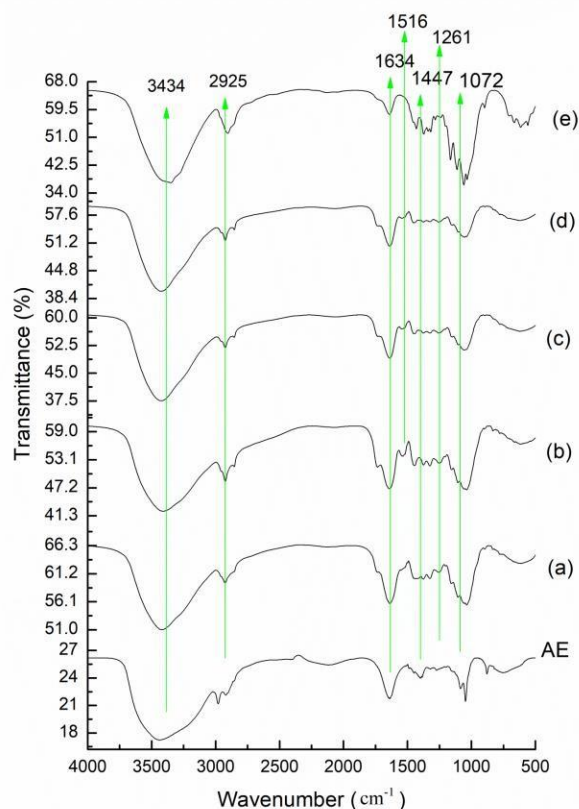


Fig. 5.3.1. FT-IR analysis of anthocyanin extract (AE) and DF-anthocyanin formulation

*(a) DF-C, (b) DF-A2, (c) DF-A3, (d) DF-A4, and (e) CEL-A

X-ray Diffraction analysis of DF-anthocyanin formulation

The degree of crystallinity (D_C) was determined from the X-ray diffraction analysis. DF-C does not exhibit any distinct peak, indicating its amorphous nature. The crystallinity of the DF-anthocyanin formulation increased after addition of anthocyanin extract and varied from 25.86-41.70%. The D_C for CEL-A was maximum (56.90%). Increased crystallinity of quercetin-fibre nanoformulation compared to the pure fibre and weaker as compared to pure quercetin was also observed by Khor et al. [49].

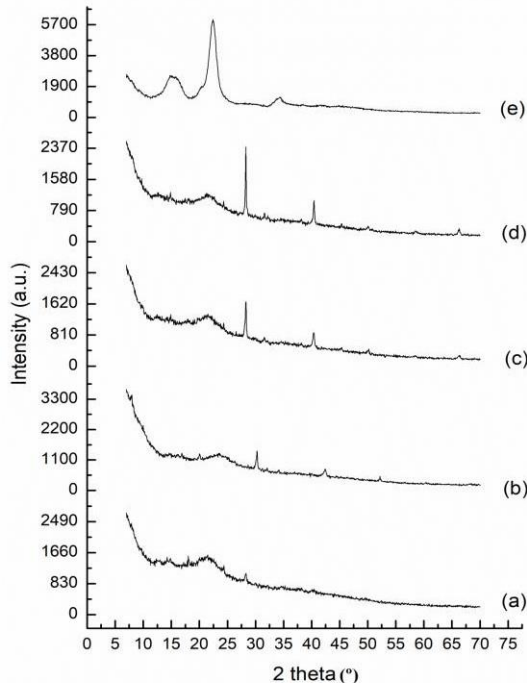


Fig.5.3.2. X-ray diffraction analysis of DF-anthocyanin formulation

Table 6: Degree of crystallinity (D_c) of DF-anthocyanin formulation

Sample Code	Degree of Crystallinity (%)
DF-C	25.86±0.07 ^a
DF-A2	28.11±0.10 ^b
DF-A3	38.32±0.21 ^c
DF-A4	41.70±0.11 ^d
CEL-A	56.90±0.20 ^e

*(Mean with different superscript letters in the same column represent a significant difference at $p < 0.05$, values represent mean ± SD; n=3)

Morphology study of DF-anthocyanin formulation

The morphology of the formulated DF-anthocyanin formulations were studied using SEM. Spherical particle of size ranges from 1.97-3.86 μm . These particles were appeared to be entrapped in network structure of DF. Surface attachment of some particles in the cellulose rod structure was observed. Similar kind of morphology was found in quercetin-fibre

nanoformulation with quercetin particles (1-5 μ m), wrapped inside the fibre outer shell. Moreover, small rod like particles (100 nm) and their agglomerates were observed on the surfaces of cellulose fibre [49].

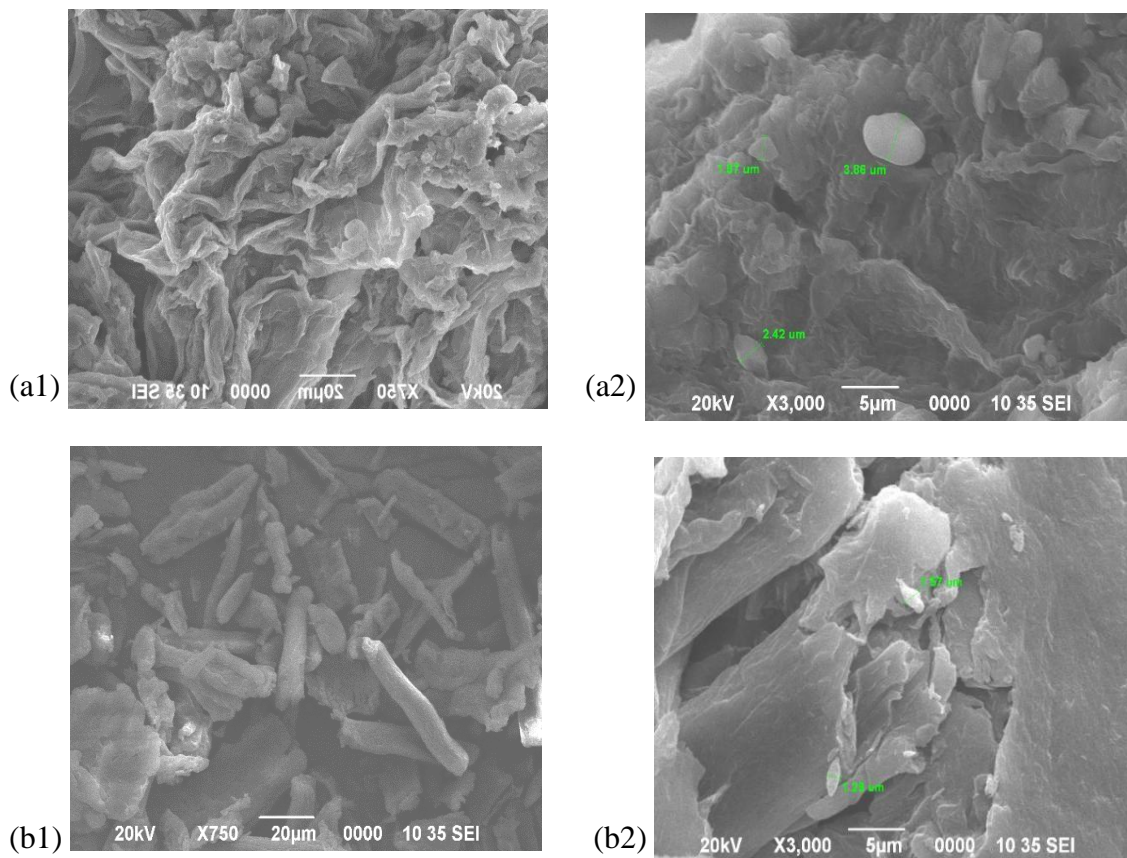


Fig. 5.3.3. SEM micrograph of DF-anthocyanin formulation (a1) DF-A3 at 750X, (a2) at 3000X; (b1) CEL-A at 750X, (b2) at 3000X

Fluorescence properties of DF-anthocyanin formulation

The fluorescence emission spectra (at pH-5.5) of anthocyanin extract, DF-C and DF-A3 were observed. Akin emission spectra ($\lambda_{exc}= 270$ nm) was observed for anthocyanin extract and DF-A3 with the maxima at 322 nm and in the visible range at 546 nm. However, the fluorescence emission intensity of the extract was significantly higher as compared to DF-A3. Besides, DF-C does not exhibit any prominent fluorescence emission band and can be regarded as non-fluorescent. Hence, the complex formation between anthocyanin extract and DF in DF-anthocyanin formulation was confirmed by fluorescence characterization

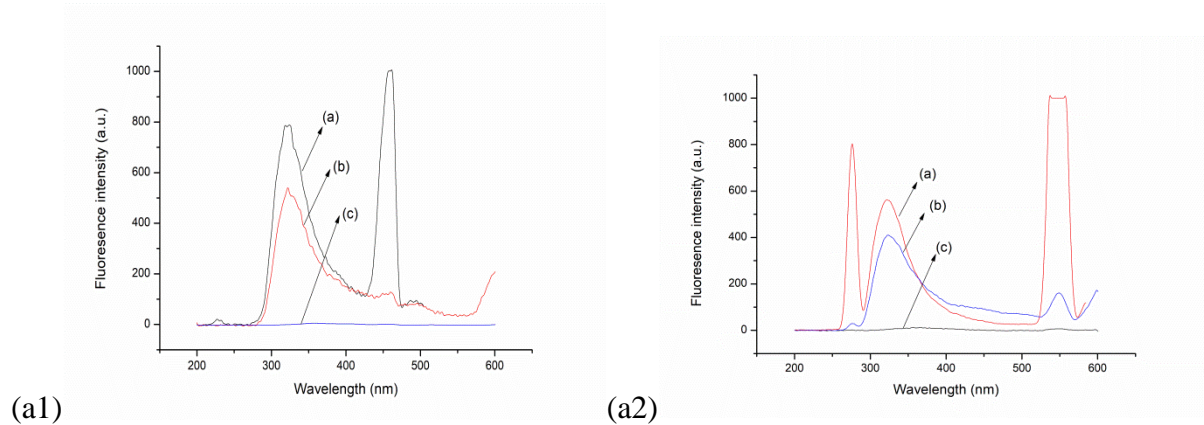


Fig.5.3.4. Fluorescence emission spectra at excitation wavelength (a1) $\lambda_{exc}= 220 \text{ nm}$; (a2) $\lambda_{exc}= 270 \text{ nm}$

*(a) Anthocyanin extract; (b) DF-A3; (c) DF-C

Anthocyanin stability of DF-anthocyanin formulation

The rate of degradation (k), half-life period ($t_{1/2}$), actual $t_{1/2}$ with R^2 values for all three kinetic reaction model was studied. Degradation of pigments and vitamin during processing or storage, generally follow first order reaction kinetics [50]. Moura et al. [51] also explained that thermal degradation of the anthocyanins can be described in terms of first order reaction kinetics. But, in our study, the best fits model (higher R^2) was found for the second order reaction kinetics. A fast degradation was observed for the first fourth week followed by gradual degradation. The fast degradation (up to fourth week) might be due the oxidation of surface anthocyanin. The lower degradation rate could be explained by limitation in oxygen transfer rate to the entrapped anthocyanin in DF matrix [14]. Moreover, the degradation was lower in DF-A3 compared to the other formulations ($k=0.0002 \text{ day}^{-1}$) with half-life period of 87 days. Thus, the formulation of DF-anthocyanin (1:3) showed better storage stability with longest half-life period.

Table 7: Degradation kinetics of the DF-anthocyanin formulation

Sample code	k (days ⁻¹)	t _{1/2} (days)	R ²	Actual t _{1/2} (days)
Zero order				
DF-A2	0.1224	61.25	0.6428	59.50
DF-A3	0.2768	75.32	0.9129	77.49
DF-A4	0.2570	55.16	0.7092	40.67
CEL-A	0.1442	63.56	0.7728	65.94
First order				
DF-A2	0.0121	56.98	0.8559	59.50
DF-A3	0.0087	79.03	0.9681	77.49
DF-A4	0.0145	47.51	0.8974	40.67
CEL-A	0.0113	61.11	0.9225	65.94
Second order				
DF-A2	0.0041	56.56	0.9506	59.50
DF-A3	0.0002	87.57	0.9786	77.49
DF-A4	0.0007	46.48	0.9616	40.67
CEL-A	0.0008	62.44	0.9818	65.94

Objective 4: Stability study of the encapsulated anthocyanin powder

Encapsulation efficiency

In order to evaluate the effectiveness of microencapsulation, TA and surface anthocyanin (SA) contents of the microparticles were determined after spray drying. For TA determination, 100 mg of samples were weighed in an amber vial with a screw top and about 1 ml of distilled water was added and was ground to destroy the microparticles. Ethanol (9 ml) was added and the samples were extracted for 5 min and then filtered. For determination of SA, 100 mg of samples was directly extracted with 10 ml ethanol and vortexed for 30 s, followed by centrifugation (SIGMA Laborzentrifugen, 3–18 KS, Osterode, Germany) at 3,000 rpm for 10 min. After phase separation, the clear supernatant was collected and filtered. Anthocyanin content for TA and SA

values was determined using the pH-differential method [2]. Encapsulation efficiencies were calculated according to an equation modified from Barbosa et al.[42] and shown as follows:

$$\% \text{ Efficiency} = [(TA - SA) \div TA] \times 100$$

SEM analysis

Particle structures of the spray-dried powder microparticles were evaluated by SEM (JEOL JSM-6390 LV, Japan, PN junction type, semiconducting detector). Powders of microparticles were attached to a double sided adhesive tape on SEM stubs, coated with 3–5 mA palladium under vacuum, and were examined at 20 kV and magnification of 2000X and 5000X.

Storage stability

Pigment powders were stored in ziplock bags inside an airtight container and storage study was conducted at 30°C and 75% RH using saturated salt (NaCl) solution for a period of 21 days and the effects of storage on anthocyanin contents, antioxidant activity, moisture content, and colour characteristics of the powder were analysed at every 7-day interval.

Anthocyanin content and DPPH radical scavenging activity

TA content was determined as referred in the preceding subhead “Encapsulation efficiency”. DPPH scavenging activity of the extract of powder was estimated by the method of Luo et al. [52]. α -Tocopherol was used as the standard antioxidant compound. Briefly, 50 mg of the extracted powder was dissolved in 5 ml of methanol solution and shaken in an incubator shaker at 150 rpm at 25°C for 30 min. The filtered mixture of methanolic extract (2 ml) was mixed with 2 ml of methanolic solution containing 0.1 mM DPPH. The reaction mixture was mixed vigorously and kept in dark for 30 min and the absorbance was recorded at 517 nm.

Moisture content

The moisture content of the anthocyanin encapsulated powder material was determined according to Association of Official Analytical Chemists (AOAC) [18]. The sample (2 g) was placed in a previously dried (at 105°C for 1 h) empty moisture estimation box. The aluminium box was dried in an oven at 105°C until constant weight was attained. After drying, the aluminium box was removed from the oven and cooled in a desiccator and the weight was taken after reaching room temperature. The loss in weight was taken as the moisture loss of the samples and was calculated using the following relationship:

$$\% \text{Moisture} = (\text{Loss of weight} - \text{weight of sample}) \times 100$$

Colour characteristics

The effect of storage on the colour characteristics of the encapsulated anthocyanin powder was analysed after every 7 days of interval. L*, a*, and b* colour values of the encapsulated anthocyanin powder were measured using a Hunter Color Measurement Spectrophotometer (UltraScan VIS, Hunter Lab). Equipment standardization was carried out by placing a black card inside the transmission compartment, and then placing distilled water (as clear liquid) in a cell over the transmission port and a white standard tile at the reflectance port. After standardization the L*, a*, and b* values were measured. Powders (0.5 g) were dissolved completely in 25 ml of distilled water and subjected to a colorimeter in a 1.0 cm path length optical glass cell and the CIE L*, a*, and b* values were measured in total transmission mode, using illuminant C and 10° observer angle.

Statistical analysis

Experiments were carried out in triplicate and the means of data obtained were evaluated using Duncan's multiple range test to identify significant differences at the 0.05 probability ($p < 0.05$) using SPSS 16.

Results and discussion

Encapsulation efficiency

The efficiency of encapsulated anthocyanin was analysed. Robert et al. [53] reported that the encapsulation efficiencies of maltodextrin-encapsulated pomegranate juice and maltodextrin-encapsulated pomegranate ethanol extract ranged between 89.4–100 and 96.7–100%, respectively. The encapsulation efficiency of encapsulated powder in this study was found in this range and therefore encapsulated powder with good encapsulation efficiency was obtained. Encapsulation efficiencies are also related to the shelf life of the anthocyanin content in the powder [54].

Particle size and microstructure

The particles of powder that were spray dried at 170°C air inlet temperature with 20°Brix feed solid levels evinced the particle size ranged from 2 to 10 µm approximately. The spray-dried capsules containing maltodextrins looked like smooth spheres but were not uniform, showing minimum agglomeration and dents on the surface, more porous structure, and were well distributed. Similar surface morphology was also observed in the SEM analysis of microencapsulated barberry's anthocyanin [13]. SEM analysis of the spray-dried powders of

black carrot anthocyanin pigments containing various wall materials showed the particle size ranging from 3 to 20 μm approximately with a smooth spherical shape [55]. SEM structures also elucidated that the particle size of the microencapsulated anthocyanin pigment present in *Garcinia indica* ranged from 5 to 50 μm with smooth spheres and are in line with the present study [56].

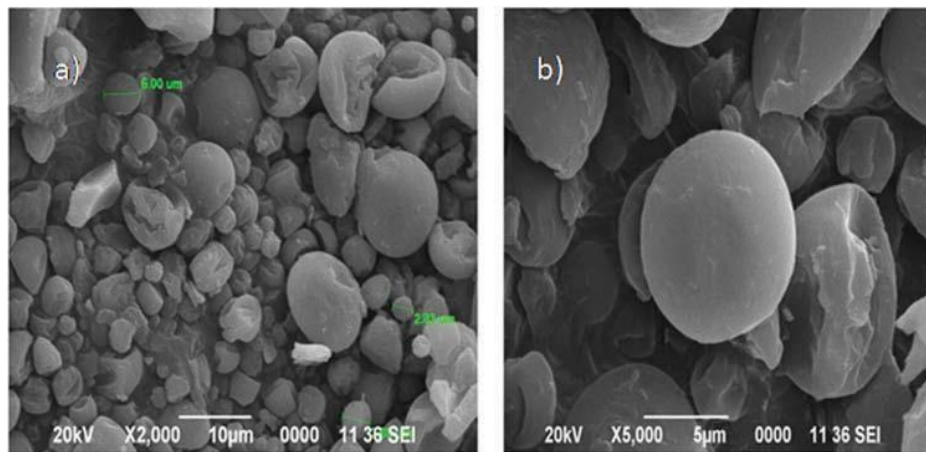


Fig.3. SEM micrographs of anthocyanin-encapsulated spray-dried powder: a) 2000X and b) 5000X.

Storage stability

Stability of anthocyanin, antioxidant activity, moisture content, and colour changes in spray-dried microencapsulated powders stored at 30°C and 75% RH for a period of 21 days were evaluated after every 7 days of interval.

Anthocyanin content

The anthocyanin content of encapsulated pigment powder decreased gradually and decreased by 44% at the end of 21 days at 30°C and 75% RH. The increase of temperature led to a faster anthocyanin degradation, since these pigments are highly thermo-sensitive. This negative influence of temperature on anthocyanin stability has been observed by many researchers. Pacheco-Palencia et al. [57] evaluated the anthocyanin stability in the whole, semi-clarified, and clarified açai pulp, and verified a degradation rate 3.5 times higher when the samples were stored at 20°C compared to a storage temperature at 4°C. Ersus and Yurdagel [55] studied the stability of microcapsules of black carrot anthocyanin and verified a loss of 33% after 64 days of storage at 25°C, whereas at 4°C the loss was 11%. The faster anthocyanin degradation at higher temperature can also be related to the presence of sugars and proteins, which can result in the

Maillard reaction, and generally occurs during food processing at high temperatures or during food storage for a long time.

DPPH radical scavenging activity

The antioxidant activity of spray-dried pigment powder decreased with prolongation in storage period and decreased by 8.4% at the end of 21 days of storage. A slow initial decline of antioxidant activity was also mentioned by Bhattacharjee et al. [58] in spray-dried anola powder up to 5 months (995.1–921.2 mmol g⁻¹). Decrease of the antioxidant capacity during storage might be ascribed to the decrease of anthocyanin content and was also observed in spray-dried bayberry powders [59].

Moisture content

Moisture content of the encapsulated pigment powder increased gradually and reached up to 71.8% at 21 days of storage period. The rate of moisture uptake by encapsulated pigment powder depends on the water activity inside the package headspace as well as package permeability [60]. Moreover, maltodextrin has a high number of ramifications with hydrophilic groups containing shorter chains, and thus can easily bind to water molecules from the ambient air during powder handling [13].

Colour characteristics

The initial colour parameters L*, a*, b*, C*, and H° values for encapsulated anthocyanin powder were determined. There was a gradual decrease of the lightness and red colour, visually observed in spray-dried powder during storage and verified by the similar decrease of a* and L* values. However, the increase in yellowness was observed at 7, 14, and 21 days, respectively. The changes of redness (a*) might be attributed to the degradation of anthocyanins during storage [61]. The reduction of spray-dried betacyanin pigment content during storage was also observed by a reduction in the values of a*, which indicated a decrease in red colour intensity in the stored samples [62].

Conclusion

In the present study, RSM based on CCD was successfully employed to optimize the ultrasonic-assisted extraction and 56.98 mg/100g anthocyanin was obtained. Anthocyanin extracted from banana bract under the optimum condition was further purified and two major constituents, viz. cyanidin-3-O-glucoside and peonidin-3-O-glucoside, were characterized by HPLC. The pigment powder was encapsulated by spray drying and showed acceptable hygroscopicity, suitable

solubility, and good encapsulation efficiency. Extraction of DF using UAE in combination with alkaline method improved the DF content, purity, crystallinity, reduced particle size and improved functional properties than the alkaline method alone. UEDF had higher total DF content compared to AEDF which was illustrated in its chemical composition. From GC MS analysis, different phenolics were identified the extracted fibre and in deoiled CBB. FT-IR result indicated the typical structure of polysaccharide with all functional group present in UEDF and AEDF along with deoiled CBB. More regular honeycomb structure with uniform and lesser particle size was observed in UEDF than AEDF. Crystallinity of UEDF was significantly higher as compared to AEDF. TGA analysis showed better thermal stability of UEDF compared to AEDF. The improvement in functional properties (WHC, OHC, WSC, α -AAIR, GAC) evidenced that UEDF is superior to AEDF. Thus, the present study suggests that UAE in combination with alkaline method is an efficient method for extracting DF with better yield, purity and functional properties. Moreover, the study needs to include physiological functions of the extracted DF to support its application as functional ingredients in diabetic food. The present study revealed that addition of anthocyanin in DF matrix greatly improves the anthocyanin and antioxidant content of DF-anthocyanin formulation and was highest in DF-A3. Moreover, the color values were also improved by addition anthocyanin which was summarized in the color characteristics study. No structural changes were noticed by FT-IR spectra after addition of anthocyanin in DF matrix, although the D_c increased with increase of pigment-matrix ratio as showed in X-ray diffraction analysis. The morphology study (DF-A3 and CEL-A) by SEM confirmed entrapment and surface attachment of particles (1.97-3.86 μm) in the network structure of DF. The fluorescence emission spectra of DF-anthocyanin complex confirmed the interaction between anthocyanin and DF. The storage stability study showed that anthocyanin degradation of DF-anthocyanin followed second order kinetics. In addition DF-A3 showed lowest degradation with the longest half-life period relative to other formulations. Thus, the pigment-matrix ratio (3:1) was optimum for DF-anthocyanin formulation with improved antioxidant content and storage stability. Further investigation is required to obtain the information about the kind of complex formation between anthocyanin and dietary fibre in the complex. The results of the present investigation has the credentials to support that the developed DF-anthocyanin formulation (DF-A3) could be an excellent “antioxidant dietary fibre” with an interesting color and can be used as supplement or functional ingredients for value-added food

products. The DF-anthocyanin formulation (DF-A3) was further utilised for bread fortification. The present study revealed that culinary banana bract is an excellent source of anthocyanin. Particle size of the spray-dried encapsulated powder was found in the range of 2–10 µm with a smooth spherical morphology as evidenced from SEM. In addition, anthocyanin content and free radical scavenging activity decreased and the moisture content increased significantly during storage at 30°C and 75% RH. Colour change as revealed by L*, a*, and b* indicated a decrease in anthocyanin stability during storage and studies on moisture sorption isotherm of the encapsulated anthocyanin powder for determining the proper storage condition will help improve its stability and in the development of value-added foods.

References

1. Zhou, J.; Zheng, X.; Yang, Q.; Liang, Z.; Li, D.; Yang, X.; Xu, J. Optimization of Ultrasonic-Assisted Extraction and Radical Scavenging Capacity of Phenols and Flavonoids from *Clerodendrum cyrtophyllum* Turcz Leaves. *Plos One* 2013, 8(7), e68392.
2. Lee, J.; Durst, R.W.; Wrolstad, R.E. Determination of Total Monomeric Anthocyanin Pigment Content of Fruit Juices, Beverages, Natural Colorants, and Wines by The PH Differential Method: Collaborative Study. *Journal of AOAC International* 2005, 88(5), 1269–1288.
3. García-Tejeda Y.V.; Salinas-Moreno, Y.; Martínez-Bustos, F. Acetylation of Normal and Waxy Maize Starches as Encapsulating Agents for Maize Anthocyanins Microencapsulation. *Food and Bioproducts Processing* 2015, 94, 717–726.
4. Cai, Y.Z.; Corke, H. Production and Properties of Spray-Dried *Amaranthus betacyanin* Pigments. *Journal of Food Science* 2000, 65(6), 1248–1252.
5. Tonon, R.V.; Brabet, C.; Rubinger, M.D. Influence of Process Conditions on the Physicochemical Properties of açai (*Euterpe oleraceae* Mart.) Powder Produced by Spray Drying. *Journal of Food Engineering* 2008, 88, 411–418.
6. Singh, J.; Singh, N. Studies on the Morphological and Rheological Properties of Granule Cold Water Soluble Corn and Potato Starches. *Food Hydrocolloids* 2003, 17, 63–72.
7. Dranca, F.; Oroian, M. Optimization of Ultrasound-Assisted Extraction of Total Monomeric Anthocyanin (TMA) and Total Phenolic Content (TPC) from Eggplant (*Solanum melongena* L.) Peel. *Ultrasonics Sonochemistry* 2016, 31, 637–646.

8. Ramić, M.; Vidović, S.; Zeković, Z.; Vlačić, J.; Cvejin, A.; Pavlič, B. Modeling and Optimization of Ultrasound-Assisted Extraction of Polyphenolic Compounds from *Aronia melanocarpa* by-products from Filter-Tea Factory. *Ultrasonics Sonochemistry* 2015, 23, 360–368.
9. Handa, S.S.; Khanuja, S.P.S.; Longo, G.; Rakesh, D.D. *Extraction Technologies for Medicinal and Aromatic Plants*. Trieste: ICS UNIDO, 2008, 1–266.
10. Barnes, J.S.; Nguyen, H.P.; Shen, S.; Schug, K.A. General Method for Extraction of Blueberry Anthocyanins and Identification Using High Performance Liquid Chromatography-Electrospray Ionization-Ion Trap-Time of Flight-Mass Spectrometry. *Journal of Chromatography A* 2009, 1216, 4728–4735.
11. Pazmino-Duran, A.; Giusti, M.M.; Wrolstad, R.E.; Gloria, M.B.A. Anthocyanin from Banana Bract (*Musa X paradisiaca*) as Potential Food Colorant. *Food Chemistry* 2001, 73, 327–332.
12. Ferrari, C.C.; Germer, S.P.M.; Alvim, I.D.; Vissotto, F.Z.; Mauricio, J. Influence of Carrier Agents on the Physicochemical Properties of Blackberry Powder Produced by Spray Drying. *International Journal of Food Science and Technology* 2012, 47, 1237–1245.
13. Mahdavi, A.S.; Jafari, M.S.; Assadpoor, E.; Dehnada, D. Microencapsulation Optimization of Natural Anthocyanins with Maltodextrin, Gum Arabic and Gelatin. *International Journal of Biological Macromolecules* 2016, 85, 379–385.
14. Tonon, R.V.; Brabet, C.; Hubinger, M.D. Anthocyanin Stability and Antioxidant Activity of Spray-Dried Acai (*Euterpe oleracea* Mart.) Juice Produced with Different Carrier Agents. *Food Research International* 2010, 43 (3), 907–914.
15. Avaltroni, F.; Bouquerand, P.E.; Normand, V. Maltodextrin Molecular Weight Distribution Influence on the Glass Transition Temperature and Viscosity in Aqueous Solutions. *Carbohydrate Polymers* 2004, 58, 323–324.
16. Kanha, N.; Laokuldilok, T. Effects of Spray-Drying Temperatures on Powder Properties and Antioxidant Activities of Encapsulated Anthocyanins from Black Glutinous Rice Bran. *Food and Applied Bioscience* 2014, 13(1), 411–423.
17. Ma, M. and Mu, T. Effects of extraction method and particle size distribution on the structural, physicochemical, and functional properties of dietary fibre from deoiled cumin. *Food Chemistry*, 194: 237-246, 2016.

18. AOAC. *Official Methods of Analysis of AOAC International*. AOAC International, Gaithersburg, Maryland, USA, 19th edition, 2012.
19. Prosky, L., Asp, N. G., Schweizer, T. F., De Vries, J. W., and Furda, I. Determination of insoluble, soluble and total dietary fibre in foods and food products: Collaboration study. *Journal - Association of Official Analytical Chemists*, 71: 1017-1023, 1998.
20. Cleven, R., Van der Berg, C., and Van Der Plas, L. Crystal structure of hydrated potato starch. *Starch/Starke*, 30: 223-228, 1978.
21. Zhang, W., Zeng, G., Pan, Y., Chen, W., Huang, W., Chen, H., and Li, W. Properties of soluble dietary fibre-polysaccharide from papaya peel obtained through alkaline or ultrasound-assisted alkaline extraction. *Carbohydrate Polymers*, 172: 102-112, 2017.
22. Guentas, L., Pheulpin, P., Michaud, P., Heyraud, A., Gey, C., Courtois, B., and Courtois, J. Structure of a polysaccharide from a Rhizobium species containing 2-deoxy- β -D-arabino-hexuronic acid. *Carbohydrate Research*, 332: 167-173, 2001.
23. Lv, J. S., Liu, X. Y., Zhang, X. P., and Wang, L. S. Chemical composition and functional characteristics of dietary fibre-rich powder obtained from core of maize straw. *Food chemistry*, 227: 383-389, 2017.
24. Rodríguez, R., Jimenez, A., Fernandez-Bolanos, J., Guillen, R., and Heredia, A. Dietary fibre from vegetable products as source of functional ingredients. *Trends in Food Science and Technology*, 17: 3-15, 2006.
25. Robertson, J. A., de Monredon, F. D., Dysseleer, P., Guillon, F., Amado, R., and Thibault, J. Hydration properties of dietary fibre and resistant starch: a European collaborative study. *LWT - Food Science and Technology*, 33: 72-79, 2000.
26. Peerajit, P., Chiewchan, N., and Devahastin, S. Effects of pretreatment methods on health-related functional properties of high dietary fibre powder from lime residues. *Food Chemistry*, 132(4): 1891-1898, 2012.
27. Ahmad, A., Anjum, F.M., Zahoor, T., Nawaz, H., and Din, A. Physicochemical and functional properties of barley β -glucan as affected by different extraction procedures. *International Journal of Food Science and Technology*, 44(1): 181-187, 2009.
28. Lopez-vargas, J. H., Fernandez-Lopez, J., Perez-Alvarez, J. A., and Viuda-Martos, M. Chemical, Physicochemical, technological, antibacterial and antioxidant properties of dietary fibre powder obtained from yellow passion fruits (*Passiflora edulis* var. flavicarpa)

- co-products. *Food Research International*, 51: 759-763, 2013.
29. Reis, S. F., Coelho, E., Coimbra, M. A., and Abu-Ghanna, N. Improved efficiency of brewer's spent grain arabinoxylans by ultrasound-assisted extraction. *Ultrasonics Sonochemistry*, 24: 155-164, 2015.
 30. Heleno, S. A., Martins, A., Queiroz, M. J. R. P., and Ferreira, I. C. F. R. Bioactivity of phenolic acids: metabolites versus parent compounds: a review. *Food Chemistry*, 173: 501–513, 2015.
 31. ChEBI. 4-Methoxycinnamic Acid. Retrieved on 9 Aug. 2019 from <http://www.ebi.ac.uk/chebi/searchId.do?chebiId=CHEBI:48541>.
 32. Janes, D., Kantar, D., Kreft, S., and Prosen, H. Identification of buckwheat (*Fagopyrum esculentum Moench*) aroma compounds with GC-MS. *Food Chemistry*, 112: 120–124, 2008.
 33. Tao, Y. J. Study on the Modification and Application of Wheat Bran Dietary Fibre. Jiangnan University, Wuxi, 2008.
 34. Pelissari, F., Sobral, P. A., and Menegalli, F. Isolation and characterization of cellulose nanofibres from banana peels. *Cellulose*, 21: 417-432, 2014.
 35. Tsalakgas, D., Lagana, R., Poljansek, I., Oven, P., and Csoka, L. Fabrications of bacterial cellulose thin films self assembled from sonochemically prepared nanofibrils and its characterization. *Ultrasonics Sonochemistry*, 28: 136-143, 2016
 36. Ahmad, F., Sairam, S., and Urooj, A. *In vitro* hypoglycaemic effects of selected dietary fibre sources. *Journal of Food Science and Technology*, 48: 285-289, 2011.
 37. Rosatella, A. A., Simeonov, S. P., Fradea, R. F. M., and Afonso, C. A. M. 5-Hydroxymethylfurfural (HMF) as a building block platform: Biological properties, synthesis and synthetic applications. *Green Chemistry*, 13: 754, 2011.
 38. Antal, M. J. J., Mok, W. S., and Richards, G. N. Mechanism of formation of 5-(hydroxymethyl)-2-furaldehyde from D-fructose and sucrose. *Carbohydrate Research*, 199: 91-109, 1990.
 39. Fernando, F., Maria, L. H., Ana-Maria, E., Chifelle, I., and Asenjo, F. Fibre concentrates from apple pomace and citrus peel as potential source for food enrichment. *Food Chemistry*, 91: 395-401, 2005.
 40. Wen, Y., Niu, M., Zhang, B., Zhao, S., and Xiong, S. Structural characteristics and

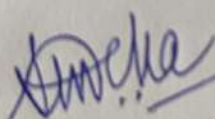
- functional properties of rice bran dietary fiber modified by enzymatic and enzyme-micronization treatments. *LWT - Food Science & Technology*, 75: 344-351, 2017.
41. Gomez-Ordóñez, E., Jiménez-Escrig, A., and Ruperez, P. Dietary fibre and physicochemical properties of several edible seaweeds from northwestern Spanish coast. *Food Research International*, 43: 2289-2294, 2010.
 42. Yalegama, L. L. W. C., Karunarante, D. N., Sivakanesan, R., and Jayasekara, C. Chemical and functional properties of fibre concentrates obtained from by-products of coconut kernel. *Food Chemistry*, 141: 124-130, 2013.
 43. AOAC. *Official Methods of Analysis of AOAC International*. AOAC International, Gaithersburg, Maryland, USA, 19th edition, 2012.
 44. Brand-Williams, W., Cuvelier, M. E., and Berset, C. Use of a free-radical method to evaluate antioxidant activity. *LWT-Food Science Technology*, 28(1): 25-30, 1995.
 45. Drabent, R., Pliszka, B., Huszcza-Ciołkowska, G., and Smyk, B. Ultraviolet fluorescence of cyanidin and malvidin glycosides in aqueous environment. *Spectroscopy Letters*, 40:165-182, 2007.
 46. Desobry, S. A., Netto, F. M., and Labuza, T. P. Comparison of spray-drying, drum-drying and freeze-drying for β -carotene encapsulation and preservation. *Journal of Food Science*, 62(6): 1158-1162, 1997.
 47. Zhao, X. Y., Chen, J., Chen, F. L., Wang, X. C., Zhu, Q. J., and Ao, Q. Surface characterization of corn stalk superfine powder studied by FT-IR and XRD. *Colloids and Surface B: Biointerfaces*, 104: 207-212, 2013.
 48. Favaro, L. I. L., Balcão, V. M., Rocha, L. K. H., Silva, E. C., Jr, J. M. O., Vila, M. M. D. C., and Tubino, M. Physicochemical characterization of a crude anthocyanin extract from the fruits of Jussara (*Euterpe edulis* Martius): Potential for Food and Pharmaceutical Applications. *Journal of Brazilian Chemical Society*, 29(10): 2072-2088, 2018.
 49. Khor, C. M., Ng, W. K., Chan, K. P., and Dong, Y. Preparation and characterization of quercetin/dietary fibre nanoformulations. *Carbohydrate Polymers*, 161: 109-117, 2017.
 50. Moura, S. C. S. R., Tavares, P. E. R., Germer, S. P. M., Nisida, A. L. A. C., Alves, A. B., and Kanaan, A. S. Degradation kinetics of anthocyanin of traditional and low sugar blackberry jam. *Food and Bioprocess Technology*, 5: 2488-2496, 2012.
 51. Moura, S. C. S. R., Berling, C. L., Germer, S. P. M., Alvim, I. D., and Hubinger, M. D.

- Encapsulating anthocyanins from *Hibiscus sabdariffa* L. calyces by ionic gelation: Pigment stability during storage of microparticles. *Food Chemistry*, 241: 317-327, 2018.
52. Luo, W.; Zhao, M.; Yang, B.; Ren, J.; Shen, G.; Rao, G. Antioxidant and Antiproliferative Capacities of Phenolics Purified from *Phyllanthus emblica* L. Fruit. *Food Chemistry* 2011, 126, 277–282.
 53. Robert, P.; Tamara, G.; Nalda, R.; Elena, S.; Jorge, C.; Carmen, S. Encapsulation of Polyphenols and Anthocyanins from Pomegranate (*Punica granatum*) by Spray Drying. *International Journal of Food Science and Technology* 2010, 45, 1386–1394.
 54. Idham, Z.; Muhamad, I.; Setapar, S.H.M.; Sarmidi, M.R. Effect of Thermal Processes on Roselle Anthocyanins Encapsulated in Different Polymer Matrices. *Journal of Food Processing and Preservation* 2011, 36, 176–184.
 55. Ersus, S.; Yurdagel, U. Microencapsulation of Anthocyanin Pigments of Black Carrot (*Daucus carota* L.) by Spray Drier. *Journal of Food Engineering* 2007, 80(3), 805–812.
 56. Nayak, C.A.; Rastogi, N.K. Effect of Selected Additives on Microencapsulation of Anthocyanin by Spray Drying. *Drying Technology* 2010, 28(12), 1396–1404.
 57. Pacheco-Palencia, L.A.; Hawken, P.; Talcott, S.T. Phytochemical, Antioxidant and Pigment Stability of Açai (*Euterpe oleracea* Mart.) as Affected by Clarification, Ascorbic Acid Fortification and Storage. *Food Research International*, 2007, 40(5), 620–628.
 58. Bhattacharjee, A.K; Tandon.; D.K.; Dikshit, A. Antioxidant Activity and Quality of Spray Dried Anola Powder as Affected by Storage Behavior of Juice. *Journal of Scientific and Industrial Research* 2014, 73, 607–612.
 59. Fang, Z.; Bhandari, B. Effect of Spray Drying and Storage on the Stability of Bayberry Polyphenols. *Food Chemistry* 2011, 129, 1139–1147.
 60. Koç, B.; Sakin-Yılmaz, M.; Kaymak-Ertekin, F.; Balkır, P. Moisture sorption isotherms and storage stability of spray-dried yogurt powder. *Drying Technology* 2010, 28, 816–822.
 61. Mahdavee Khazaei, K.; Jafari, S.M.; Ghorbani, M.; Hemmati Kakhki, A. Application of Maltodextrin and Gum Arabic in Microencapsulation of Saffron Petal's Anthocyanins and Evaluating their Storage Stability and Color. *Carbohydrate Polymers* 2014, 105, 57–62.
 62. Diaz, F.; Santos, E.M.; Filardo, S.; Villagómez, R.; Schein-Var, L. Colorant Extraction from a Red Prickly Pear (*Opuntia lasiacantha*) for Food Application. *Electronic Journal of Environmental, Agricultural and Food Chemistry* 2006, 5, 1330–1337.

1. Certified that the amount of Rs 46,767.00 mentioned against col. 9 has been utilized on the project / scheme for the purpose for which it was sanctioned and that the balance of Rs 14,806.00 remaining unutilized at the end of the year may be allowed to be carried forward to the next financial year 2021-2022 and will be adjusted towards the grants-in-aid payable during the next year.
2. Certified that I have satisfied myself that the conditions on which the grants-in-aid was sanctioned have been duly fulfilled / are being fulfilled and that I have exercised the following checks to see that the money was actually utilised for the purpose for which it was sanctioned.

Kinds of checks exercised:

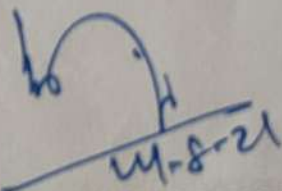
1. Cash Book
2. Ledger Book
3. Stock Book



(PROJECT INVESTIGATOR)

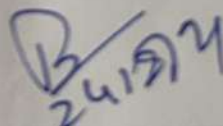
Professor

Department of Food Eng. & Technology
Tezpur University
Napaam, Tezpur- 784028, Assam



(FINANCE OFFICER)

Finance Officer
Tezpur University



(HEAD OF THE INSTITUTE)

Registrar
Tezpur University

UTILISATION CERTIFICATE
(For the financial year 01.4.2020 to 31.3.2021)

(Rs. in lakhs)

1.	Title of the project/scheme:	Valorization of Culinary Banana Flower: Waste to Value Addition Using Green Technologies
2.	Name of the Organization	Tezpur University, Assam
3.	Principal Investigator:	Prof. S.C. Deka
4.	ASTEC Letter No and date of sanctioning the project	ASTEC/S&T/1614/5/2/2017-18/853-860 Dated 19.02.2018
	Date of Start of the Project	19.02.2018
5.	Head of account as given in the original sanction letter	
6.	Amount brought forward from the previous F.Y 2019-2020:	Rs 6,767.00 (Including SL No 8)
7.	Amount received during the F.Y 2020-2021 (ASTEC/S&T/1614/5/2/2017-18/853-860 Dated 19.02.2018)	Rs 40,000.00
8.	Amount of interest accrued, if any, from the grants during F.Y 2019-2020	Rs 180 (Included in SL No 6)
9.	Total amount that was available for expenditure during the F.Y 2020-2021 (Excluding Commitments) During the F.Y (SL No 6+7+8):	Rs 46,767.00
10.	Actual expenditure (excluding commitments) incurred during the financial year F.Y 2020-2021 (up to 31.3.2020):	Rs 31,961.00
11.	Balance amount available at the end of the F.Y 2020-2021:	Rs 14,806.00
12.	Unspent balance refunded, if any (Please give details of cheque No. etc.):	NIL
13.	Amount allowed to be carried forward to the next financial year 2021-2022	Rs 14,806.00

**Statement of Expenditure Accounts
For the Financial Year 2020-2021**

- a) Title of the project/scheme: Valorization of Culinary Banana Flower: Waste to Value Addition Using Green Technologies
 b) Sanctioned letter no & date: ASTEC/S&T/1614/S/2/2017-18/853-860 Dated 19.02.2018
 c) Principal Investigator: Prof. Sankar Chandra Deka
 d) Total sanctioned cost of the project in Rs 2,00,000.00
 e) Grant Received in F.Y 2018-2019: Rs 160000.00
 f) Grant Received in F.Y 2019-2020: NIL
 g) Grant Received in F.Y 2020-2021: Rs 40,000.00

Sl No	Sanctioned Heads	Funds sanctioned for 1 st & 2 nd year	Funds carried forward from Previous year	Funds released (F.Y 2020-2021)	Funds available (iv +v)	Expenditure incurred during the F.Y. 2020-2021	Balance (vi-vii)	Commitments	Total expenditure (vii + ix)
i	ii	iii	iv	v	vi	vii	viii	ix	x
(a)	Staff	-	-	-	-	-	-	-	-
(b)	Equipment	-	-	-	-	-	-	-	-
(c)	Operation & Maint	-	-	-	-	-	-	-	-
(d)	Expendables								
	Consumables	1,60,000.00	-473.00	32,000.00	31,527.00	31,961.00	434		
	Raw materials	20,000.00	0.00	4,000.00	4,000.00	-	4000.00		
(e)	Travel	20,000.00	7,060.00	4,000.00	11,060.00	-	11,060.00		
(f)	Contingencies	-	-	-	-	-	-	-	-
(g)	Research Consultant	-	-	-	-	-	-	-	-
(h)	Procured Service	-	-	-	-	-	-	-	-
	Institutional overhead	-	-	-	-	-	-	-	-
	Interest earned (F.Y.2019-2020)	-	180.00	-	180	-	180.00		
	Total	2,00,000.00	6,767.00	40,000.00	46,767.00	31,961.00	14,806.00		31,961.00

Sancha
 (PROJECT INVESTIGATOR)
 (Signed and stamped)

Professor
 Department of Food Eng. & Technology
 Tezpur University
 Mahaganj, Tezpur- 784028, Assam

B. S. Deka
 (HEAD OF THE INSTITUTE)
 (Signed and stamped)

Registrar
 Tezpur University

h. J.
 (FINANCE OFFICER)
 (Signed and stamped)

Finance Officer
 Tezpur University